Mechanical Systems and Signal Processing (1996) **10**(5), 561–577

EXPERIMENTAL ROBOT IDENTIFICATION USING OPTIMISED PERIODIC TRAJECTORIES

J. Swevers,† C. Ganseman, J. De Schutter and H. Van Brussel

Katholieke Universiteit Leuven, Department of Mechanical Engineering, Division Production Engineering, Machine Design and Automation (PMA), Celestijnenlaan 300B, B-3001 Heverlee, Belgium

(*Received June* 1995, *accepted November* 1995)

This paper describes a new approach to the parameterisation of robot excitation trajectories for optimal robot identification. The trajectory parameterisation is based on finite Fourier series. The coefficients of the Fourier series are optimised for minimal sensitivity of the identification to measurement disturbances, which is measured as the condition number of a regression matrix, taking into account motion constraints in joint and Cartesian space. This approach allows small condition numbers with few coefficients for each joint to be obtained, which simplifies the optimisation problem significantly.

The periodicity of the resulting trajectories and the fact that one has total control over their frequency content are additional features of the presented parameterisation approach. Further optimisation of the excitation experiments is possible through time domain data-averaging and optimal selection of the excitation bandwidth, which both help to reduce the disturbance level on the measurements, and therefore improve the identification accuracy. Application of the method for the identification of the KUKA IR/361 industrial robot proves the validity of the proposed approach.

1. INTRODUCTION

Accurate robot control and realistic robot simulation require an accurate dynamic robot model. The design of an advanced robot controller, such as a computed torque or a computed velocity controller is based on the robot model, and its performance depends directly on the model accuracy [3, 9, 15, 16]. Robot simulation without a dynamic robot model cannot provide realistic execution time estimates, for example, in the case of spot-welding operations, where the time required to stop the robot end effector at the different spot-welding places depends on the robot dynamics.

Experimental robot identification is the only efficient way to obtain accurate robot models as well as indications of their accuracy, confidence and validty. The data provided by the robot manufacturers are insufficient, inaccurate, or often non-existant, especially those dealing with friction and compliance characteristics. Direct measurement of the physical parameters is unrealistic because of the complexity of most robots.

Reliable, accurate, and efficient robot identification requires specially designed experiments. When designing an identification experiment for a robot manipulator, it is essential to consider whether the excitation is sufficient to provide accurate and fast parameter estimation in the presence of disturbances. The influence of disturbances, such as measurement noise and unmodeled actuator dynamics (such as friction), on the

† Senior Research Assistant with the N.F.W.O. (Belgium National Fund for Scientific Research).

0888–3270/96/050561 + 17 $18.00/0

parameter estimates depends directly on the condition (number) of the set of equations that generate the parameters [5, 7]. The condition of this set of equations depends on the excitation during the identification experiment.

The generation of a robot trajectory that optimises the condition of the parameter estimation involves non-linear optimisation with motion constraints (i.e. constraints on joint positions, velocities, and accelerations). Several approaches have been presented. The main difference between these approaches lies in the parameterisation of the excitation trajectory. The parameters that describe the excitation trajectory are the degrees of freedom (dof) of the optimisation problem. Armstrong [1] describes an approach in which the dof are the elements of a sequence of joint accelerations. This approach is the most general one, but requires a large number of dof, such that optimisation is cumbersome. Moreover, motion constraints are difficult to satisfy. Gautier [4] optimises a linear combination of the condition number and the so-called equilibrium of the set of equations that generate the parameters. The dof are a finite set of joint angles and velocities separated in time. The actual trajectory is continuous and smooth, and calculated by interpolating a line between the optimised points, assuming zero initial and final acceleration and using a fifth-order polynomial. Motion constraints can be satisfied. Otani and Kakizaki [11] use trajectories which are a combination of a cosine and a ramp, such that the joint velocities change sinusoidally between zero and their maximum value. Excitation is optimised by carefully selecting the frequency and amplitude of the sinusoidal movements for each joint and the initial robot configuration in a rather *ad hoc* way.

This paper presents a new approach to the parameterisation of robot trajectories. It combines the advantages of the method described in [4] with new interesting features. The excitation trajectory for each joint is a finite sum of harmonic sine and cosine functions, i.e. a finite Fourier series. The amplitude of the sine and cosine functions are the dof that have to be optimised. This approach guarantees bandlimited periodic trajectories and therefore allows:

(1) Time domain data-averaging, which improves the signal-to-noise ratio of the experimental data. This is extremely important since motor current (torque) measurements, which are used in robot identification, are very noisy. Data averaging allows the data records to be compressed before they are used in the parameter estimation. This significantly reduces the number of calculations involved in the parameter estimation.
(2) Estimation of the characteristics of the measurement noise [13]. This information is valuable in case of maximum-likelihood parameter estimation.
(3) Specification of the bandwidth of the excitation trajectories, such that excitation of the robot flexibility can be either completely avoided or intentionally brought about.
(4) Calculation of joint velocities and accelerations from the measured response in an analytical way. For this purpose, the measured encoder readings are first approximated, in a least squares sense, as a finite sum of sine and cosine functions. This corresponds to taking the discrete Fourier transform of the encoder readings and selecting the main spectral lines. The Fourier transform does not introduce leakage errors because of the periodicity of the excitation. This frequency domain approach towards the differentiation of time series is simple, efficient, and accurate.

None of the existing methods possess the above mentioned features with the result that:

(1) Large data records, which are necessary in order to obtain reliable parameter estimates, cannot be compressed and result in large overdetermined sets of equations which require large numbers of calculations to be solved.

(2) The calculation of joint velocities and accelerations requires complex numerical differentiation techniques or specially designed IIR filters [14]. This approach is less accurate than the exact frequency domain approach which is only possible if the excitation is periodic.
(3) Estimation of the noise characteristics requires extra experiments.
(4) Special precautions have to be taken, for example filtering of the excitation trajectory, in order to avoid excitation of the robot flexibility.

Extending the length of a Fourier series to infinity allows approximation of any arbitrary periodic function, while non-periodic functions can be approximated arbitrarily close if non-harmonic sine and cosine functions are allowed in the Fourier series. In this sense, the method presented in this paper approximated Armstrong's approach [1], but has the advantage that motion constraints can be met. Moreover, simulation results show that Fourier series with only a few harmonic sine and cosine functions for each joint are sufficient to reduce the condition number of the set of equations that generate the parameters to small values, such that there is no need for more dof in the parameter space and to allow arbitrary trajectories.

The following section describes the least squares estimation of the parameters of a dynamic robot model, and discusses the influence of the robot trajectory on the sensitivity of the parameter estimates to disturbances. Section 3 describes the parameterisation of the excitation trajectories and formulates the constrained optimisation problem which generates the optimal Fourier coefficients. Section 4 illustrates the presented approach through the experimental identification of a KUKA IR/361 industrial robot.

2. LEAST SQUARES ROBOT PARAMETER ESTIMATION

The following set of n differential equations describes the dynamic behavior of an n dof rigid robot [15]:

$$\mathbf{M}(\mathbf{q})\ddot{\mathbf{q}} + \mathbf{f}(\mathbf{q}, \dot{\mathbf{q}}) = \boldsymbol{\tau}, \tag{1}$$

where $\mathbf{q}$ is the n-vector of the joint angles, $\mathbf{M}$ the $n \times n$ mass matrix (which is a function of the joint angles), $\mathbf{f}$ the n-vector which specifies the gravitation, Coriolis, viscous and Coulomb friction effects, and $\boldsymbol{\tau}$ the n-vector of the actuator torques. The parameters related to the mass distribution and the friction coefficients are the unknown parameters that have to be estimated. The dynamic model is linear in the friction coefficients as well as in the parameters of the mass distribution if they are combined in the so-called barycentric parameters [2]. In that case, the dynamic model (1) can be rewritten as a set of linear equations:

$$\boldsymbol{\Phi}(\mathbf{q}, \dot{\mathbf{q}}, \ddot{\mathbf{q}})\boldsymbol{\theta} = \boldsymbol{\tau}. \tag{2}$$

$\boldsymbol{\Phi}(\mathbf{q}, \dot{\mathbf{q}}, \ddot{\mathbf{q}})$ is the $n \times r$ regressor matrix, depending on the joint angles, velocities, and accelerations. r is the number of independent robot parameters. $\boldsymbol{\theta}$ is the r-vector containing the unknown barycentric parameters and friction coefficients.

Robot identification deals with the problem of estimating the model parameters $\boldsymbol{\theta}$ from the response measured during a robot excitation experiment. In most cases, the data obtained from an experiment is a sequence of joint angles and motor currents, from which a sequence of joint velocities, accelerations, and motor torques are calculated. These data are entered in equation (2), yielding a regressor matrix $\boldsymbol{\Phi}(\mathbf{q}_k, \dot{\mathbf{q}}_k, \ddot{\mathbf{q}}_k)$ and vector $\boldsymbol{\tau}_k$ for each

sample instant k in the data sequence. Combining these matrices and vectors yields the following overdetermined set of equations:

$$\mathbf{A\theta} = \mathbf{b}, \tag{3}$$

with

$$\mathbf{A} = \begin{bmatrix} \mathbf{\Phi}(\mathbf{q}_1, \dot{\mathbf{q}}_1, \ddot{\mathbf{q}}_1) \\ \vdots \\ \mathbf{\Phi}(\mathbf{q}_M, \dot{\mathbf{q}}_M, \ddot{\mathbf{q}}_M) \end{bmatrix} \quad \text{and} \quad \mathbf{b} = \begin{bmatrix} \boldsymbol{\tau}_1 \\ \vdots \\ \boldsymbol{\tau}_M \end{bmatrix},$$

where M represents the length of the data sequence.

The parameter vector, $\boldsymbol{\theta}$, can be estimated as the linear least squares solution $\boldsymbol{\theta}_{ls}$ of this overdetermined set of equations:

$$\boldsymbol{\theta}_{ls} = \arg\min_{\boldsymbol{\theta}} \|\mathbf{A\theta} - \mathbf{b}\|_2^2 = \mathbf{A}^+\mathbf{b}, \tag{4}$$

where $\|\cdot\|_2$ represents the 2-norm of a vector and $\mathbf{A}^+$ the pseudo inverse of the matrix $\mathbf{A}$ [5].

The condition number of matrix $\mathbf{A}$, cond ($\mathbf{A}$), is a measure of the sensitivity of the least squares solution, $\boldsymbol{\theta}_{ls}$, to perturbations on the elements of $\mathbf{A}$ and $\mathbf{b}$, provided that the matrix is well equilibrated [4, 5, 7]. Normalisation of matrix $\mathbf{A}$, i.e. the division of the columns of $\mathbf{A}$ by their norm, assures equilibration. The condition number of the normalised matrix, $\mathbf{A}$, is therefore taken as the criterion to design the excitation experiment: the robot trajectory during the excitation experiment should be such that the condition number of the normalised matrix $\mathbf{A}$ is minimal, without violating the motion constraints. The calculation of such a trajectory is a complex constrained non-linear optimisation problem, which can be solved using sequential quadratic programming methods, which are available in commercially available software packages such as Matlab [6]. The complexity of the optimisation problem depends on the motion constraints and the parameterisation of the trajectory. This paper presents a novel approach to trajectory parameterisation, which allows small condition numbers with few parameters to be obtained.

Gautier [4] improves the equilibration of $\mathbf{A}$ by multiplying the columns of $\mathbf{A}$ with *a priori* available values of their respective parameters. This reduces the identification problem to the estimation of multiplicative corrections to the *a priori* available parameter values. With respect to the calculation of the excitation trajectory, this different approach to the parameter estimation only changes the regressor matrix of which the condition number has to be minimised. The trajectory parameterisation presented in the following section can be applied to both approaches without changing the optimisation algorithm.

3. PARAMETERISATION OF THE ROBOT EXCITATION TRAJECTORY

The angular position, q_i, velocity, $\dot{q}_i$, and acceleration, $\ddot{q}_i$, trajectories for joint i of a n dof robot are finite Fourier series:

$$q_i(t) = \sum_{l=1}^{N_i} \frac{a_l^i}{\omega_f l} \sin(\omega_f l t) - \frac{b_l^i}{\omega_f l} \cos(\omega_f l t) + q_{i0}$$

$$\dot{q}_i(t) = \sum_{l=1}^{N_i} a_l^i \cos(\omega_f l t) + b_l^i \sin(\omega_f l t)$$

$$\ddot{q}_i(t) = \sum_{l=1}^{N_i} -a_k^i \omega_f l \sin(\omega_f l t) + b_l^i \omega_f l \cos(\omega_f l t), \tag{5}$$

with ω_f the fundamental pulsation of the Fourier series. This Fourier series specifies a periodic function with period $T_f = 2\pi/\omega_f$. The fundamental pulsation is common for all joints, in order to preserve the periodicity of the overall robot excitation. Each Fourier series contains $2 \times N_i + 1$ parameters that constitute the dof for the optimisation problem: a_l^i, and b_l^i, for $l = 1$ to N_i, which are the amplitudes of the cosine and sine functions, and q_{i0} which is the robot configuration around which the robot excitation occurs. For simplicity of notation, we consider that the vector $\boldsymbol{\delta}$ contains these parameters for all joints.

The Fourier series for each joint consists of a fundamental frequency and $N_i - 1$ harmonic frequencies. The number of harmonic frequencies determines the bandwidth of the trajectory. Certain harmonic frequencies can be omitted from the Fourier series. This allows restriction of the energy of the trajectory within a specific frequency band, or avoid excitation within a certain frequency band. The choice of the fundamental pulsation ω_f depends on (a) the desired period of the excitation, and is therefore related to the duration of the experiment; and (b) the minimum frequency resolution of the excitation trajectory, which is $\omega_f/2\pi$.

This trajectory parameterisation approach allows the frequency content (frequency resolution and bandwidth) of the excitation to be controlled, which is extremely important if the excitation of the robot flexibility must be either completely avoided or intentionally brought about.

The optimisation constraints are limitations on the joint angles, velocities, and accelerations, and on the robot end effector position in the Cartesian space in order to avoid collision with the environment or the robot itself. This last type of constraint involves forward kinematics calculations. All constraints are implemented as continuous functions which are negative if the constraint is satisfied and positive if it is violated. Section 4 gives an example of these constraints.

The following expression gives the mathematical formulation of this constrained optimisation problem:

$$\hat{\boldsymbol{\delta}} = \arg\min_{\delta} \operatorname{cond}(\mathbf{A}(\boldsymbol{\delta}, \omega_f)),$$

$$\text{with} \begin{cases} \mathbf{q}_{\min} \leqslant \mathbf{q}(pT_s, \boldsymbol{\delta}) \leqslant \mathbf{q}_{\max} \\ -\dot{\mathbf{q}}_{\max} \leqslant \dot{\mathbf{q}}(pT_s, \boldsymbol{\delta}) \leqslant \dot{\mathbf{q}}_{\max} \\ -\ddot{\mathbf{q}}_{\max} \leqslant \ddot{\mathbf{q}}(pT_s, \boldsymbol{\delta}) \leqslant \ddot{\mathbf{q}}_{\max} \\ \{\mathbf{s}(\mathbf{q}(pT_s, \boldsymbol{\delta}))\} \subset \mathbf{S} \end{cases}$$

$$\text{for} \quad 0 \leqslant p \leqslant \frac{T_f}{T_s}, \tag{6}$$

with T_s the sampling period for the data acquisition during the experiment. The fundamental pulsation ω_f of the trajectories is fixed. Its value depends on the desired frequency spectrum and the data acquisition capacity. The constraints in (6) are element-wise inequalities. $\mathbf{q}_{\min}$, $\mathbf{q}_{\max}$, $\dot{\mathbf{q}}_{\max}$, and $\ddot{\mathbf{q}}_{\max}$ are the vectors containing the minimum (min), and maximum (max) joint angle, velocity and acceleration values. $\mathbf{S}$ represents the available working space of the robot. $\{\mathbf{s}(\mathbf{q})\}$ represents the set of end effector positions resulting from the joint trajectories, using forward kinematics calculation.

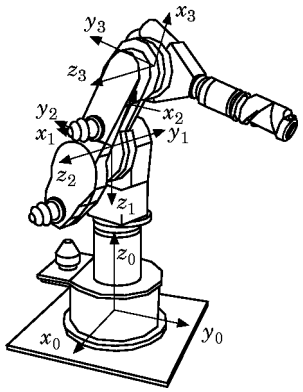

Figure 1. Schematic representation of a KUKA IR/361 industrial robot.

4. EXPERIMENTAL VERIFICATION

This section illustrates the presented trajectory parameterisation through its application on a KUKA IR/361 industrial robot, which is a manipulator with 6 rotational dof. Figure 1 shows the robot, its base co-ordinate system (x_0, y_0, z_0), and coordinate systems for the first three links: (x_i, y_i, z_i), $i = 1, 2, 3$. First, the trajectory generation method is applied to a 1 dof model of the third robot axis. Various data processing approaches are compared in detail. Secondly, the trajectory generation method is applied to a 3 dof model of the first three axes of the KUKA IR/361. In all experiments, links 4, 5, and 6 (i.e. the links constituting the robot wrist) are fixed with respect to link 3, i.e. with respect to coordinate system (x_3, y_3, z_3), their configuration being that of a fully stretched wrist. As a result, the wrist is considered as part of link 3, and the inertial parameters related to links 4, 5, and 6 are added to the corresponding parameters of link 3.

4.1. EXPERIMENTAL IDENTIFICATION OF THE THIRD AXIS OF A KUKA IR/361

4.1.1. *Model for the third axis*

The following equation shows the 1 dof model for the third axis of the KUKA IR/361 robot (Fig. 2):

$$\tau_3(t) = (I_{3zz} + m_3(l_{3x}^2 + l_{3y}^2))\ddot{\theta}_3(t) - m_3 g l_{3x} \sin(\theta_3(t)) + m_3 g l_{3y} \cos(\theta_3(t)) + V_3\dot{\theta}_3(t) + C_3 \operatorname{sign}(\dot{\theta}_3(t)) \quad (7)$$

Remember that since the robot wrist is fixed, it is considered as part of link 3.

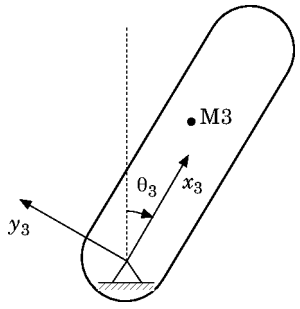

Figure 2. Schematic representation of axis 3.

The reduced model contains five parameters: three of them are a combination of the 10 inertial parameters of the third link, two correspond to the friction model:

(1) $I_{3zz} = m_3(l_{3x}^2 + l_{3y}^2)$ (kgm^2): the inertia of link 3 referred to the rotation axis 3. I_{3zz} is the moment of inertia around the z-axis (the z-axis is parallel with the rotation axis 3 and perpendicular to the $x3$- and $y3$-axis shown in Fig. 2) through the centre of gravity (COG) of link 3. l_{3x} and l_{3y} are the x and y co-ordinates of the COG in the local frame ($x3$, $y3$, $z3$) of link 3. m_3 is the mass of link 3.
(2) $m_3 l_{3x}$ (kgm): product of the mass of link 3 and the X co-ordinate of the COG of link 3 with respect to the local frame ($x3$, $y3$, $z3$).
(3) $m_3 l_{3y}$ (kgm): product of the mass of link 3 and the Y co-ordinate of the COG of link 3 with respect to the local frame ($x3$, $y3$, $z3$).
(4) V_3 (Nms/rad): viscous friction coefficient.
(5) C_3 (Nm): Coulomb friction coefficient.

4.1.2. *Trajectory optimisation for the third axis*

Equation (7) is linear in the five unknown parameters, and can therefore be reformulated as a set of linear equations, like equation (2). Entering the data obtained from a robot excitation experiment into equation (2) yields an overdetermined set of equations like equation (3). The robot excitation trajectories, parameterised according to equation (5), are optimised such that the condition number of the normalised matrix **A** in equation (3) is minimal, taking into account the motion constraints for the robot.

The motion constraints are limitations on the joint angles, velocities, and accelerations, and on the robot end effector position in the Cartesian space in order to avoid collision with the ceiling of the laboratory. The following limitations are specified by the robot control and measurement system [17]:

(1) joint angle limits (rad): $-2.3 < q_3 < 2.3$;
(2) joint velocity limits (rad/s): $-1.45 < \dot{q}_3 < 1.45$;
(3) joint acceleration limits (rad/s^2): $-3 < \ddot{q}_3 < 3$;
(4) limits on the height of the end effector (mm): $500 < z_{ee} < 2500$. z_{ee} is the height of the end effector above the ground and results from forward kinematics calculations.

The excitation trajectories are five-term Fourier series (five harmonics with different amplitude and phase, and one DC component), yielding 11 trajectory parameters. The fundamental frequency of the trajectory is 0.1 Hz. The sampling rate is 150 Hz, yielding data vectors with a length of 1500 data samples per period.

The constrained optimisation is performed using the "CONSTR" function of the Optimisation Toolbox of Matlab [6]. This function uses a sequential quadratic programming method.

The condition number of the normalised matrix **A** [equation (3)] that results from these trajectories is three. Figure 3 shows the optimised excitation trajectory.

4.1.3. *Identification and model validation*

The robot is driven under velocity control with analog joint controllers to maintain the desired velocity. Data is collected after the transient response of the robot has died out. The joint angle is measured by means of an encoder mounted on the motor shaft, and the actuator torque is measured indirectly by means of the motor current. An analog eighth-order low-pass filter projects the sampling of the motor current signal from aliasing errors. This filtering introduces amplitude and phase distortions, which are corrected by filtering the sampled motor current sequence with the inverse of the digital equivalent of the analog

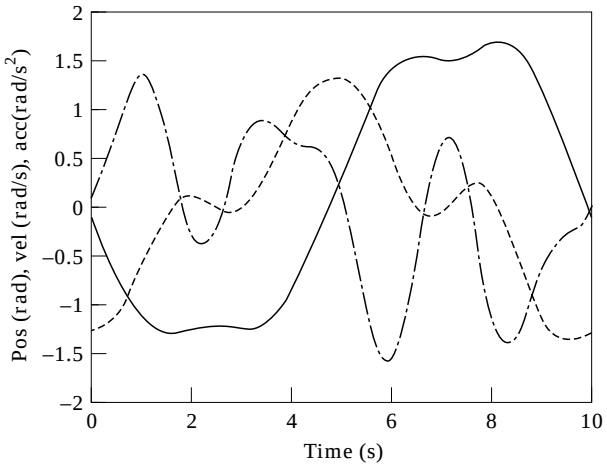

Figure 3. Optimised excitation trajectory for axis 3, position or angle (——), angular velocity (– – –), angular acceleration (—·—·—·).

filter. Subsequently, the data sequences are averaged over 16 periods in order to improve the signal-to-noise ratio of the measurements.

Identification of the dynamic robot model requires joint velocity and acceleration data. Direct numerical differentiation of the measured joint position data yields noisy velocity and acceleration data, which makes accurate parameter estimation impossible. This paper suggests two different approaches in order to improve the signal-to-noise ratio of the velocity and acceleration data:

Approach I: The measured position can be approximated by a finite Fourier series containing the same limited set of frequencies as the desired position. Figure 4 shows the estimation residue of this approximation. Velocity and acceleration are calculated in an analytical way as the derivatives of the obtained limited Fourier series.

Approach II: Due to the periodicity of the measurements, the velocity and acceleration can be calculated in the frequency domain after Fourier transform without introducing

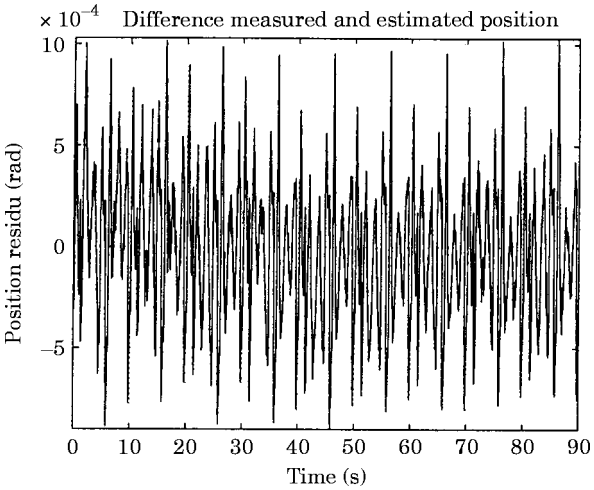

Figure 4. Estimation residue for the 1 dof model of axis 3 for the excitation trajectory.

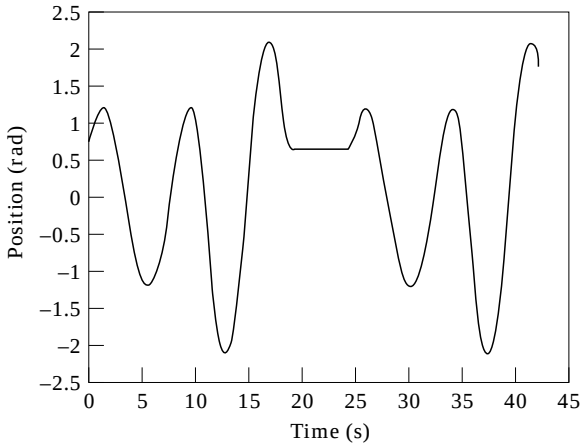

Figure 5. Validation trajectory for axis 3.

leakage errors. Inverse Fourier transform gives the velocity and acceleration in the time domain. A similar approach is to calculate the acceleration and velocity via special digital filters [14]. This approach results, however, in very noisy acceleration data. Filtering the columns of matrix **A** and matrix **b** [equation (3)] with a digital low-pass filter reduces the signal noise. The best results were obtained with a second order Butterworth filter with cut-off frequency of 5 Hz.

Remark: Direct measurement of joint velocity by means of the tachometer signal is a valuable alternative to the calculation of the time derivative of the encoder measurement, provided that the tachometer signal can be calibrated (from volts to rad/s) sufficiently accurately. The joint accelerations can then be calculated by means of the first derivative of the tachometer signal, however, resulting in very noisy acceleration signals if numerical differentiation techniques are applied. It is expected that the signal-to-noise ratio of the thus obtained joint accelerations is comparable to that of joint accelerations obtained from numerical differentiation of position encoder measurements. Hence, it is still better to use the suggested Approaches I and II in the case of tachometer signals.

To verify the model accuracy, position and motor current are measured from a validation trajectory which is different from the excitation trajectory. Figure 5 shows the validation trajectory. It contains parts with constant acceleration, parts with zero velocity and a 13th-order polynomial. The measured motor torque is compared with the torque calculated using the measured motion data, the model and the estimated model parameters.

Table 1 shows the estimated parameter values resulting from the two motion data processing approaches mentioned above, and the corresponding mean-squared torque residues for the validation trajectory. The mean-squared residue is the mean of the squared difference between the measured and calculated motor torque for the validation trajectory.

Table 1 shows that both signal processing approaches yield similar results. Figure 6 shows the measured and simulated torque for the excitation and the validation trajectory using the model parameters resulting from Approach II. The largest estimation errors appear when the robot velocity is zero. The friction model containing only Coulomb and viscous friction is not accurate enough for low velocities. Especially the non-linear Coulomb term that causes small errors in the estimated velocity result in large torque errors at low velocities.

TABLE 1

Estimated parameters of the third axis model corresponding to Approach I and II, and the resulting mean-squared residue for the validation trajectory

Parameter	Units	Frequency domain differentiation approach	Finite Fourier series approach
inertia	kgm^2	8.348	8.402
mb_{3x}	kgm	26.2	26.13
mb_{3y}	kgm	−0.02349	−0.2163
V_3	Nms/rad	3.676	4.339
C_3	Nm	15.8927	15.2116
mean squared residue (val. traj.)	$(Nm)^2$	5.788	5.932

4.2. EXPERIMENTAL IDENTIFICATION OF THE FIRST THREE AXES OF A KUKA IR/361

4.2.1. *Model for the first three axes*

The model for the first three axes of the KUKA IR/361 robot can be reduced to 15 independent identifiable inertial parameters [2, 10], six friction parameters (viscous and Coulomb friction parameters for each joint), and parameters that model the spring which compensates the gravitation for the second link. Section 4.2.2 describes the modeling of this gravity-compensation spring. Section 4.2.3 describes the trajectory optimisation for the 3 dof model. Section 4.2.4 describes the identification and model validation.

4.2.2. *Modelling of a gravity-compensation spring*

In order to reduce the load due to gravity on the actuator of the second link, a gravity compensation spring is mounted between the first and the second link (Fig. 7).

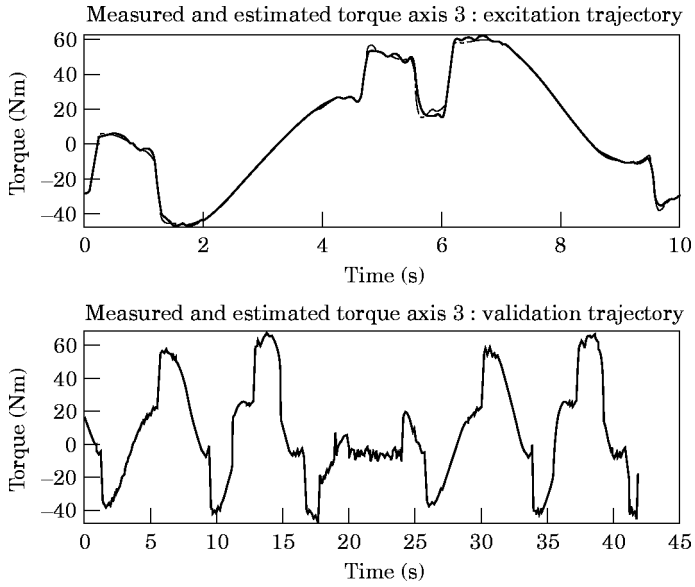

Figure 6. Measured (——) and simulated (– – –) torque for the 1 dof model for axis 3: excitation and validation trajectory.

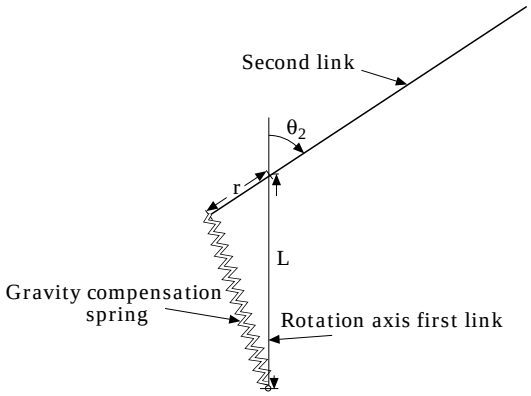

Figure 7. Mounting of gravity compensation spring.

The torque induced by the linear spring is equal to:

$$T_{spring} = \frac{Lk(\sqrt{L^2 + r^2 - 2Lr\cos(\theta_2)} - l_0)r\sin(\theta_2)}{\sqrt{L^2 + r^2 - 2Lr\cos(\theta_2)}}. \tag{8}$$

L is the distance between rotation axis 2 and the mounting of the spring on the first link, r is the distance between the rotation axis 2 and the mounting of the spring on the second link, k is the stiffness of the spring, l_0 is the length of the unloaded spring and θ_2 is the angle of the second link. Figure 8 shows the simulated torque (as a function of θ_2) due to gravitation and for the spring model shown in Fig. 7. The spring parameters (k, r, L and l_0) are calculated such that gravity compensation is nearly exact for $\theta_2 = 90^\circ$. The

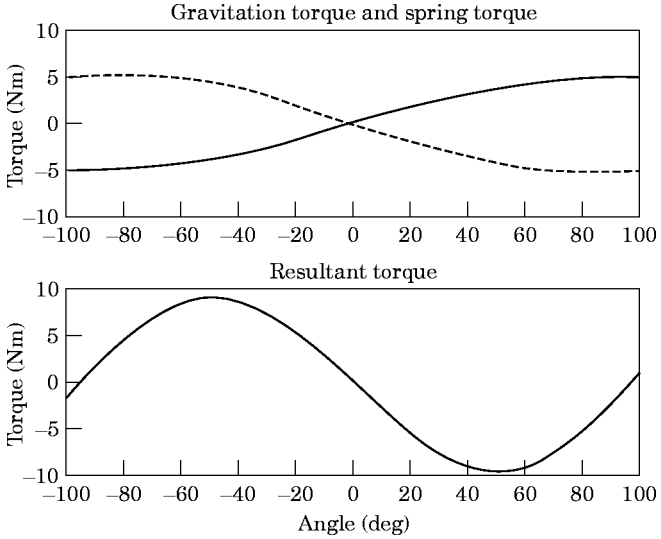

Figure 8. Gravitation and spring torque (upper figure) and the resulting sum of both torques (lower figure).

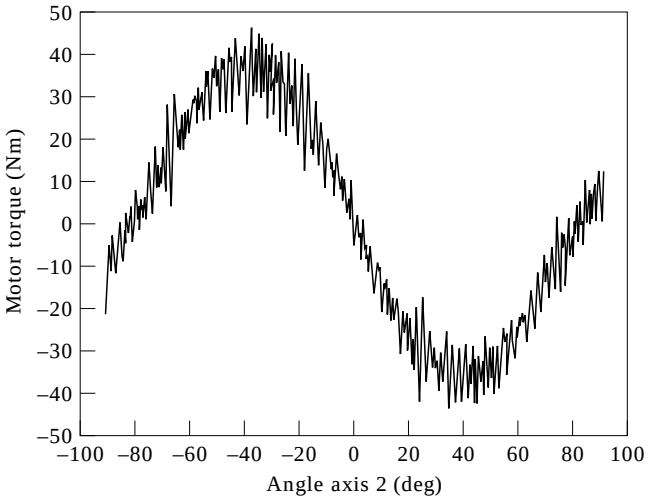

Figure 9. Measured motor torque for axis 2 as a function of the angular position of axis 2.

resulting torque (Fig. 8) can be approximated by a sum of harmonically related sine and cosine functions:

$$T_{resulting} = \sum_{l=1}^{\infty} A_l \cos(l\theta_2) + B_l \sin(l\theta_2) \tag{9}$$

The second harmonic ($l = 2$) is the main component. Measurements on the KUKA robot confirm this behaviour: Fig. 9 shows the actuator torque for axis 2 as a function of θ_2 when the robot is fully stretched. This measurement shows that the spring compensates gravity almost exactly for $\theta_2 = 90^\circ$.

The torque, T_{spring}, is non-linear in the parameters L and r. This non-linear dependency and the low sensitivity of T_{spring} for changes in its parameters, makes the estimation of the spring parameters from noisy data cumbersome. A better approach is to approximate the resulting torque as a finite Fourier series [equation (9)] and estimate the Fourier coefficients A_l and B_l. An approximation with three harmonics gives an accurate estimate of the motor torque for the considered robot. This extends $\boldsymbol{\theta}$ [equation (2)] to a 25×1 column vector and $\boldsymbol{\Phi}$ to a 3×25 matrix.

4.2.3. *Trajectory optimisation for the first three axes*

The optimisation of the excitation trajectory has been performed in the same way as for the 1 dof model. The excitation trajectories are five-term Fourier series, yielding 11 parameters for each joint. The fundamental frequency of the trajectories is 0.1 Hz. The sampling rate is 150 Hz. The length of the data sequence is 1500 data samples per period of the trajectory. The motion constraints for the trajectory optimisation, which are specified by the measurement system, are:

(1) joint angle limits (rad): $-1.6 < q_1 < 1.6$, $-1.2 < q_2 < 1.2$, and $-2.3 < q_3 < 2.3$,
(2) joint velocity limits (rad/s): $-1.45 < \dot{q}_i < 1.45$,
(3) joint acceleration limits (rad/s^2): $-3 < \ddot{q}_i < 3$,
(4) limits on the height of the end effector (mm): $500 < z_{ee} < 2500$,
(5) the robot touches its base if $r_{ee} < 700$ mm and $z_{ee} < 1800$ mm. r_{ee} is the distance of the end effector from the first robot axis. z_{ee} is the height of the end effector above the ground. r_{ee} and z_{ee} are obtained from forward kinematics calculations.

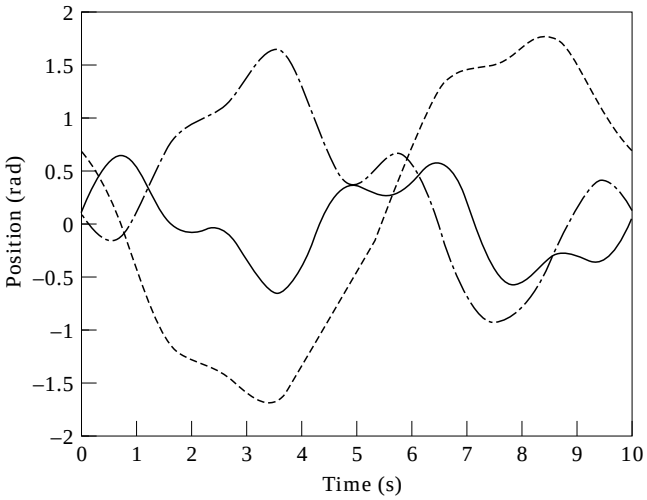

Figure 10. Optimised robot excitation trajectory (——, axis 1; – – – –, axis 2; – · – · –, axis 3).

Figure 10 shows the optimised excitation trajectories. The optimisation of the trajectory stopped when it reached a condition number equal to 47.3.

Both examples show that this parameterisation approach allows generation, with few parameters, of excitation trajectories which result in a small condition number. Although the obtained optima are not necessarily the global optima, this approach is valuable because the resulting condition numbers are sufficiently small.

4.2.4. *Identification and model validation for the first three axes*

The experiments are performed as described in Section 4.1.3. The measured joint angle and motor current data sequences are averaged over 16 periods, which improves the

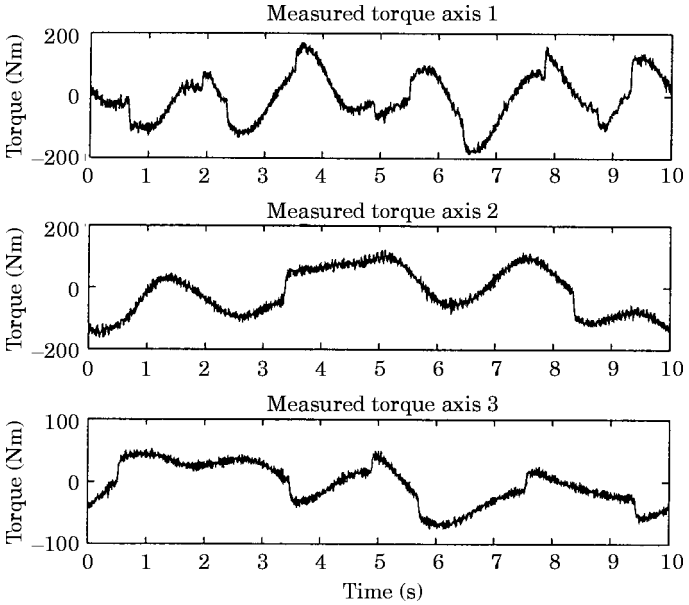

Figure 11. Measured actuator torques for the excitation trajectory.

signal-to-noise ratio of the measurements. The joint velocities and accelerations are calculated according to Approach I (see Section 4.1.3). The next paragraph motivates the preference for Approach I.

Figure 11 shows the averaged actuator torque measurements for the excitation trajectory. The variance of the noise on the averaged joint angle and actuator torque measurements is estimated by calculating the sample variance for each data point and dividing it by 16. The mean values of these estimated variance values are 4.7×10^{-11} rad^2, 3.9×10^{-11} rad^2, 9.4×10^{-10} rad^2 for the position of respectively axes 1, 2 and 3 and 49 N^{2}m^2, 54 N^{2}m^2, 7.7 N^{2}m^2 for the torque of axes 1, 2 and 3 respectively. These values show that the noise level on the position measurements is significantly smaller than the noise level on the motor torque measurements. The approximation, in least-squares sense, of the averaged measured joint angles by five-term Fourier series (Approach I) yields approximation errors of which the variances are comparable with the estimated variances of the noise on the averaged measured joint angles. Using these estimated Fourier series instead of the averaged measured joint angles corresponds to very selective noise filtering, yielding joint angle, velocity, and acceleration data, and therefore a matrix **A**, which are nearly free of noise. As a result, the condition for which the least squares solution is asymptotically unbiased, is nearly satisfied. This cannot be accomplished if Approach II is used, since data filtering (applied to all columns of matrix **A**) colours the noise, yielding biased least-squares parameter estimates. Moreover, it is well known that the identification results strongly depend on the choice of the data filter [8]. Therefore, from a theoretical and practical point of view Approach I is to be preferred.

Remark: The excitation trajectories presented by [1] and [4] cannot apply Approach I since they are non-periodic. Although experiments show that Approach II yields models of which the accuracy is comparable to the models resulting from Approach I if the data filter is appropriately chosen (see Section 4.1.3), the fact that the method of [1] and [4] cannot apply Approach I must be seen as:

(1) a theoretical disadvantage since only Approach I allows approximate satisfaction of the condition for which the least-squares solution is asymptotically unbiased, and;
(2) a practical disadvantage since the choice of an appropriate data filter is not always obvious and involves trial and error.

Figure 12 shows the estimated actuator torques and the estimation residues for the excitation trajectory. The estimated actuator torques are calculated from the estimated model parameters and the finite Fourier series which approximate the measured joint angles. The peaks in the estimation residue occur at low joint angular velocity, which indicates that the assumed friction model, which includes viscous and Coulomb friction, is too simple. It can be expected that including *stiction* in the robot model results in smaller simulation errors. Due to these modeling errors, the mean values of the squared estimation residues (96 N^{2}m^2, 85 N^{2}m^2, 19 N^{2}m^2 for axes 1, 2 and 3 respectively) are larger than the noise variances of the measured torques. Despite modeling errors (stiction, deflection in the transmissions, kinematic errors) the estimated models are accurate but biased.

The accuracy of the obtained parameter estimates can be verified for a different validation trajectory by comparing the measured torques and an estimate of these torques based on the model and the measured position data. The validation trajectory goes through 20 points randomly chosen in the workspace of the robot. The robot moves with maximum acceleration and deceleration between these points, and comes to a full stop at each point. The velocities and accelerations are calculated by means of specially-designed filters

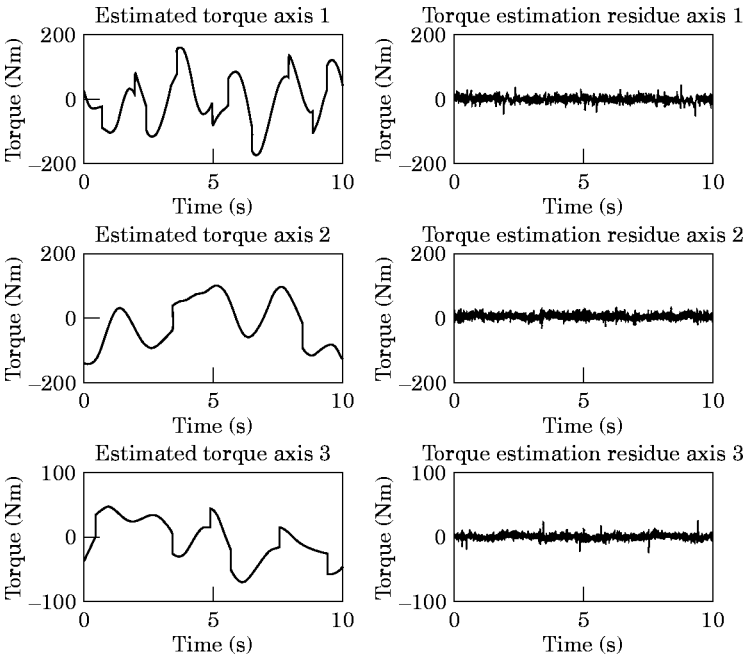

Figure 12. The estimated actuator torques, and the difference between the estimated actuator torques and the averaged actuator torque measurements for the excitation trajectory.

(Approach II) [14]. Approach I is not applicable here because the desired joint trajectories are not periodic.

Figure 13 shows the filtered actuator torque measurements for the validation trajectory. Figure 14 shows the estimated torques and the estimation residue for the validation

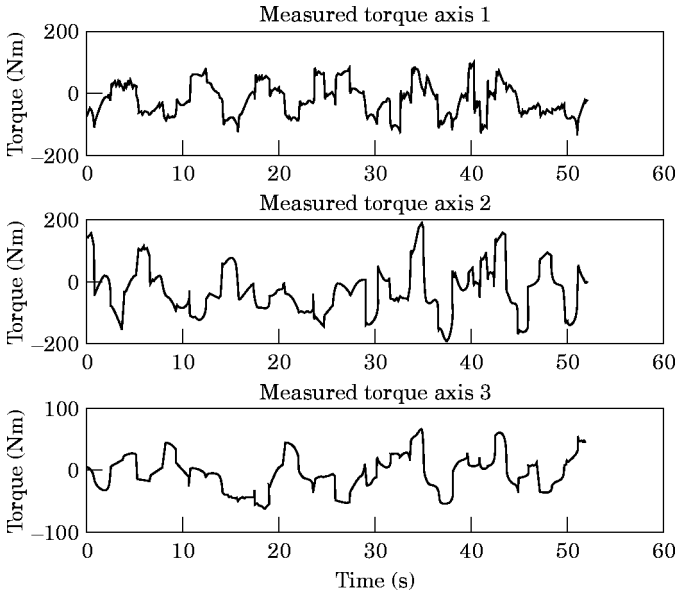

Figure 13. Measured actuator torques for the validation trajectory.

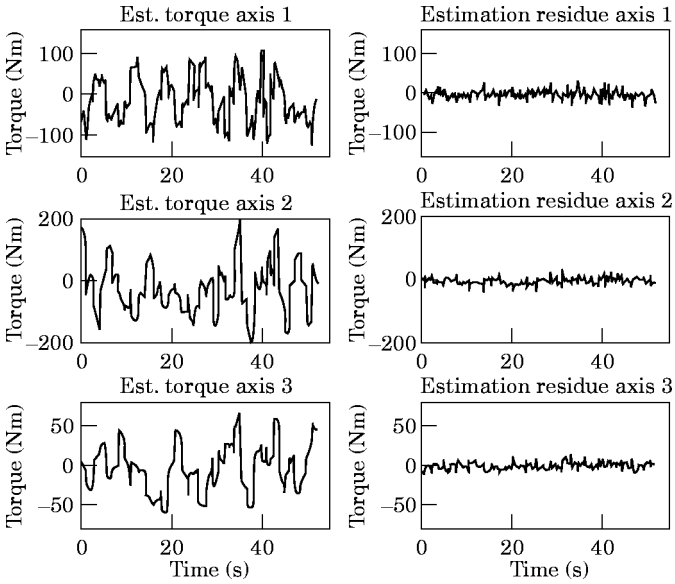

Figure 14. The estimated actuator torques, and the difference between the estimated actuator torques and the averaged actuator torque measurements for the validation trajectory.

trajectory. The torques are filtered with a low-pass filter with a cut-off frequency of 10 Hz. This reduces the noise on

(1) the measured torques, which is high due to the inverse filtering to compensate the analog filter (see Section 4.1.3) and because data-averaging is not possible here;
(2) the estimated torque due to noise on the calculated acceleration and velocity data.

The mean squared torque estimation residue for the validation trajectory is 53, 65, 15 N^2m^2 for axes 1, 2 and 3 respectively.

5. CONCLUSIONS

The presented approach to the parameterisation of robot excitation trajectories allows generation of robot experiments which are robust with respect to measurement inaccuracies. This corresponds to small condition numbers for a regression matrix defined by the set of dynamic equations. The periodicity of the trajectories allows improvement of the signal-to-noise ratio of the response data, allows calculation of the velocity or acceleration in the frequency domain, and allows approximate satisfaction of the condition for which the least squares solution is asymptotically unbiased.

Experiments on an industrial robot show that the presented trajectory generation, data processing, and least squares parameter estimation methods yield accurate, but biased, robot model parameters. It is expected that accounting for stiction, deflection in the transmission, and kinematic errors, further improves the robot model accuracy, and yields unbiased parameter estimates.

ACKNOWLEDGMENTS

This text presents research results of the Belgian programme on Interuniversity Poles of Attraction initiated by the Belgian State, Prime Minister's Office, Science Policy Programming. The scientific responsibility is assumed by its authors.

REFERENCES

1. B. Armstrong 1989 *The International Journal of Robotics Research* **8,** 28–48. On finding excitation trajectories for identification experiments involving systems with nonlinear dynamics.
2. P. Fisette, B. Raucent and J. C. Samin 1993 *Computer aided analysis of rigid and flexible mechanical systems*, *Nato-Advanced Study Institute*, **Vol. II,** 111–129. Minimal dynamic characterization of tree-like multibody systems.
3. E. Freund 1982 *International Journal of Robotics Research*, **1,** 68–78. Fast nonlinear control with arbitrary pole-placement for industrial robots and manipulators.
4. M. Gautier, C. Janin and C. Presse 1993 *Proceedings of the Second European Control Conference*, *Groningen*, *The Netherlands*, 2291–2296. Dynamic identification of robots using least squares and extended kalman filtering methods.
5. G. H. Golub and C. F. Van Loan 1989 *Matrix Computation* 2nd edn. Baltimore and London: Johns Hopkins University Press.
6. A. Grace 1992 *Optimisation Toolbox for Use with Matlab*. MA, U.S.A.: The Math Works, Inc.
7. C. L. Lawson and R. J. Hanson 1974 *Solving Least Squares Problems*. Englewood Cliffs, NJ: Prentice Hall.
8. L. Ljung 1987 *System Identification*, *Theory for the User*. Englewood Cliffs, NJ: Prentice-Hall.
9. B. Markiewicz 1973 *Analysis of computed torque drive method and comparison with conventional position servo for a computer controlled manipulator*. JPL, Caltech, TM 33–601.
10. H. Mayeda, K. Yoshida and K. Osuka June 1990 *IEEE Transactions on Robotics and Automation*, 312–321. Base parameters of manipulator dynamic models.
11. K. Otani and T. Kakizaki 1993 *Proceedings of the 24th International Symposium on Industrial Robots*, *Tokyo*, *Japan*, 743–748. Motion planning and modeling for accurately identifying dynamic parameters of an industrial robotic manipulator.
12. M. Renaud 1987 *Proceedings of the IEEE Conference on Robotics and Automation*, 1677–1682. Quasi-minimal computation of the dynamic model of a robot manipulator utilizing the Newton-Euler formalism and the notion of augmented body.
13. J. Schoukens and R. Pintelon 1991. *Identification of Linear Systems*. *A Practical Guideline to Accurate Modeling*, London: Pergamon Press.
14. R. Pintelon and J. Schoukens 1990 *IEEE Transactions on Instrumentation and Measurement* **39** (6) 923–927. Real-time integration and differentiation of analog signals by means of digital filtering.
15. M. Spong and M. Vidyasagar 1989 *Robot Dynamics and Control*. New York: John Wiley.
16. D. Torfs and J. De Schutter 1992 *Proceedings of the 23rd International Symposium on Industrial Robots*, *Barcelona*, *Spain*, 314–319. A new control scheme for a flexible robot driven by a velocity controlled actuator.
17. P. Van De Poel, W. Witvrouw, H. Bruyninckx and J. De Schutter 1993 *Proceedings of the 6th International Conference on Advanced Robotics (ICAR)*, *Tokyo*, *Japan*, 713–718. An environment for developing and optimising compliant robot motion tools.